Numerical Study of Dynamical Regimes in a Monolithic Passively Mode-Locked Semiconductor Laser

Andrei G. Vladimirov, Alexander S. Pimenov, and Dmitrii Rachinskii

***Abstract*—Bifurcation mechanisms of the development and break up of different operation regimes in a passively mode-locked monolithic semiconductor laser are studied by solving numerically partial differential equations for amplitudes of two counterpropagating waves and carrier densities in gain and absorber sections. It is shown that mode-locking regimes with different repetition rates can be multistable for a wide range of laser parameters and that the harmonic mode-locking regime with two counterpropagating pulses in the cavity can exhibit a period-doubling bifurcation leading to different amplitudes and separations of the pulses. The effect of linewidth enhancement factors in gain and absorber sections on the laser dynamics is discussed.**

***Index Terms*—Author, please supply your own keywords or send a blank e-mail to keywords@ieee.org to receive a list of suggested keywords..**

I. Introduction

PASSIVELY mode-locked semiconductor lasers emit short optical pulses with high repetition rates suitable for application in telecommunication networks [1]. The use of these pulses in modern technology implies several important limitations on their characteristics, such as pulse width, repetition frequency, amplitude noise, and timing jitter [2]. In particular, elimination of pulse amplitude noise, which appears as a result of the so-called Q-switching instability, is an important problem related to the technological application of mode-locked monolithic semiconductor lasers in telecommunication technology [3], [4]. This oscillatory instability responsible for the low-frequency (a few GHz) modulation of the amplitude of mode-locked pulses and related to the slow recovery of the intracavity gain medium can be significantly suppressed in quantum-dot lasers [5], [6]. Apart from Q-switching instability, there are other bifurcation mechanisms of the break-up of the fundamental mode-locking regime. These mechanisms can lead to the development of various dynamical regimes, such as harmonic mode-locking with a higher repetition rate than that of the fundamental mode-locking regime, irregular pulsations, and a CW operation. Numerical study of mode-locking in semiconductor lasers is in the focus of many papers (see, for example, the review paper [7] and references therein). However, only a few of them investigate bifurcation mechanisms of stabilization and destabilization of various regimes in mode-locked lasers. In particular, in [4], [8]–[12], nonlinear bifurcations in a passively mode-locked laser were studied with the help of the recently proposed ring laser model which is based on a system of delay differential equations (DDEs) and assumes the unidirectional operation approximation.

In this paper, we abandon the ring approximation and use a modification of the traveling wave model [12]–[14] describing the evolution of two counterpropagating waves in a linear laser. On the basis of the results of the work in [10], [15]–[17], an efficient numerical scheme for the solution of the traveling wave equations is constructed. This numerical scheme is used to describe typical bifurcation sequences that take place with the increase of the injection current in the gain section. We show the existence of large bistability and multistability domains and hysteresis between different dynamical regimes in a mode-locked laser. Moreover, under certain conditions, a period-doubling bifurcation of the harmonic mode-locking regime is predicted. This bifurcation leads to the coexistence of two counterpropagating pulses with different amplitudes and different time separations in the laser cavity. Finally, we investigate the effect of the linewidth enhancement factors in the gain and absorber sections on the laser dynamics and demonstrate that the amplitude-phase coupling introduced by these factors can lead to a mode-locking regime with a quasi-periodic laser intensity.

II. Model Equations

Let us consider a model of a monolithic semiconductor laser consisting of four sections (see Fig. 1): reverse-biased saturable absorber ($0 < z' < l_q$), forward-biased gain section ($l_q < z' < l_q + l_g$), phase tuning section ($l_q + l_g < z' < l_q + l_g + l_p$), which is used to adjust repetition frequency of mode-locked pulses, and a spectral filtering element [2], [3]. Here, l_g, l_q, and l_p denote the length of the gain, absorber, and passive sections, respectively. Normalized equations describing temporal and spatial evolution of the amplitudes of two counterpropagating waves $E^{\pm}$ and the carrier density N in the gain and absorber sections [18] can be written in the form

$$\frac{\partial E^{\pm}}{\partial t} \pm \frac{\partial E^{\pm}}{\partial z} = -\frac{\beta}{2}E^{\pm} + \frac{1-i\alpha}{2}NE^{\pm} \qquad (1)$$

Manuscript received September 10, 2008; revised December 06, 2008. This work was supported in part by the Science Foundation Ireland, Project SFB 787 of the DFG, and by the Russian Foundation for Basic Research under Grant 06–01-72552.

A. G. Vladimirov is with the Weierstrass Institute for Applied Analysis and Stochastics, D-10117 Berlin, Germany, and also with the Physics Faculty, St. Petersburg State University, **[AUTHOR: PLEASE PROVIDE A POSTAL CODE.—ED.]** St. Petersburg, Russia (e-mail: vladimir@wias-berlin.de).

A. Pimenov and D. Rachinskii are with the Department of Applied Mathematics, University College Cork, **[AUTHOR: PLEASE PROVIDE A POSTAL CODE.—ED.]** Cork, Ireland (e-mail: d.rachinskii@ucc.ie).

Digital Object Identifier 10.1109/JQE.2009.2013363

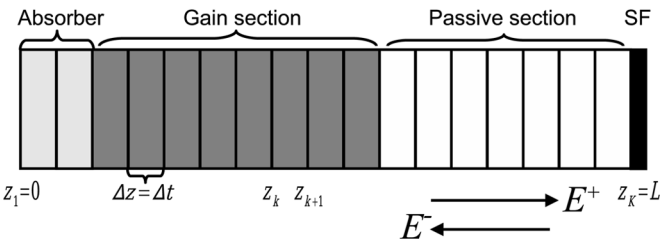

Fig. 1. Schematic representation of a model of monolithic semiconductor laser. The laser sections are split into segments of equal optical length Δz. SF: thin spectral filtering section. $E^{\pm}$: amplitudes of two counterpropagating waves.

$$\frac{\partial N}{\partial t} = N_0 - \gamma N - sN\left(|E^+|^2 + |E^-|^2\right) \quad (2)$$

where $z = z'/v$, which has the dimension of time, is the rescaled coordinate along the cavity axis and v is the group velocity of light which we assumed to be the same in both laser sections. In (1) and (2), the variables $E^{\pm}$ are dimensionless and the normalized variable $N = g\Gamma(n - n_{\rm tr})$ has the dimension of inverse time. Here $n - n_{\rm tr}$ is the excess of the carrier density over transparency level, g is the differential gain (loss) coefficient in the amplifying (absorbing) section, and Γ is the optical confinement factor. The relaxation rate β describes linear internal losses in the semiconductor material, α is the so-called linewidth enhancement factor, γ is the carrier relaxation rate, and $N_0 = g\Gamma[j/(ed) - \gamma n_{\rm tr}]$ is the unsaturated gain parameter, where j is the injection current density ($j = 0$ for the absorber section), e is the electron charge, and d is the active layer thickness. N_0 is positive in the gain section (amplification) and negative in the absorber section (absorption). The electric field envelope $E^{\pm}$ is rescaled in such a way that $s_g^{-1} = 10$ ps in the gain section and $s_q = s_g(g_q/g_g)$ in the absorber section. Here and below, the subscripts g and q are added to distinguish between the parameters of the gain and the absorber sections, respectively. In our calculations, we use the following fixed values for the parameters of the laser sections: $\gamma_q^{-1} = 1$ ns, $\gamma_q^{-1} = 10$ ps, $\beta_g^{-1} = \beta_q^{-1} = 10$ ps, $s_q^{-1} = s_g^{-1}/5 = 2$ ps, $l_g/v = 6.25$ ps, $l_q/v = 0.625$ ps, $l_p/v = 5.625$ ps, $N_{0q} = -32\gamma_q^2$. We note that the investigation of the effect of spontaneous emission on the laser dynamics lies beyond the scope of this paper. Some results concerning the influence of spontaneous emission noise on the stability of mode-locked regimes can be found in [10], [19], and [20].

Boundary conditions at the left laser facet $z = 0$ can be written in the form

$$E^+(t,0) = \sqrt{\kappa_1}E^-(t,0) \quad (3)$$

where κ_1 describes the reflectivity of the left laser facet.

Industrial samples of monolithic mode-locked lasers comprise special Bragg reflection sections that act as a spectral filter for the laser radiation. In the case when such a section is absent, the spectral filtering results from the finiteness of the spectral bandwidth of the gain section. Here, we assume that a thin spectral filtering section is located near the right laser facet. Then, the effect of this section on the laser radiation can be expressed by the boundary condition

$$E^-(t,L) = \sqrt{\kappa_2}\int_0^{\infty} f(\tau)\,E^+(t-\tau,L)\,d\tau \quad (4)$$

where κ_2 and f describe the reflectivity of the right laser facet and the form of the spectral filtering profile, and L is the total cavity length. In accordance with [8] and [10], we use the Lorentzian shape of the spectral filtering $f(t) = \delta\exp(-\delta t)$ with the bandwidth δ. In our calculations, $\kappa_1 = \kappa_2 = 0.3$ and $\delta^{-1} = 0.5$ ps.

III. Numerical Method

In order to solve (1)–(4), we apply a numerical scheme similar to that used in [16] to study active mode-locking in semiconductor lasers. First, we divide each of the laser sections into a number of segments of equal optical length $\Delta z = \Delta t$, where Δt is the time required for light to pass through this segment (see Fig. 1). Let the total number of segments be K. In each segment $z_k \le z \le z_{k+1}$ of the gain and absorber sections, we integrate (1) for the counterpropagating waves along the characteristics. The solutions are given by

$$E^+(t+\Delta z, z_{k+1}) = E^+(t,z_k) \times \exp\left[-\frac{\beta\Delta z}{2} + \frac{1-i\alpha}{2} \times \int_{z_k}^{z_{k+1}} N(t-z_k+z,z)\,dz\right] \quad (5)$$

$$E^-(t+\Delta z, z_k) = E^-(t,z_{k+1}) \times \exp\left[-\frac{\beta\Delta z}{2} + \frac{1-i\alpha}{2} \times \int_{z_k}^{z_{k+1}} N(t+z_{k+1}-z,z)\,dz\right]. \quad (6)$$

For $\Delta z \ll 1$, the two integrals in (5) and (6) can be approximated to the order of Δz^3 by a single time-dependent integral

$$G_k(t) = \int_{z_k}^{z_{k+1}} N\left(\frac{t+\Delta z}{2}, z\right)dz.$$

Using this approximation, we can rewrite the transformations (5) and (6) in the form

$$E^+(t+\Delta z, z_{k+1}) = E^+(t,z_k) \times \exp\left(\frac{1-i\alpha}{2}G_k(t) - \frac{\beta\Delta z}{2}\right) \quad (7)$$

$$E^-(t+\Delta z, z_k) = E^-(t,z_{k+1}) \times \exp\left(\frac{1-i\alpha}{2}G_k(t) - \frac{\beta\Delta z}{2}\right). \quad (8)$$

In order to obtain the equation for $G_k(t)$, we integrate (2) over the interval $z_k \le z \le z_{k+1}$ and arrive at

$$\frac{dG_k}{dt} = G_0 - \gamma G_k - s\int_{z_k}^{z_{k+1}} N\left(\frac{t+\Delta z}{2}, z\right) \times \left|E^+\left(\frac{t+\Delta z}{2}, z\right)\right|^2 dz s \int_{z_k}^{z_{k+1}} N\left(\tfrac{t+\Delta z}{2}, z\right) \times \left|E^-\left(\frac{t+\Delta z}{2}, z\right)\right|^2 dz \quad (9)$$

where $G_0 = N_0\Delta z$ is the cumulative unsaturated gain (loss) associated with the segment $z_k \le z \le z_{k+1}$ of the gain (absorber) section. The integrals in (9) can be approximated as follows. Multiplying (1) by the complex conjugate amplitudes $\bar{E}^{\pm}$ and considering the real part of the resulting equations, we obtain

$$\frac{\partial|E^{\pm}|^2}{dt} \pm \frac{\partial|E^{\pm}|^2}{\partial z} = (-\beta + N)\,|E^{\pm}|^2.$$

Integration of these equations along the characteristics leads to

$$|E^+(t+\Delta z, z_{k+1})|^2 - |E^+(t, z_k)|^2 = \int_{z_k}^{z_{k+1}} \left[N(t - z_k + z, z) - \beta\right] \times |E^+(t - z_k + z, z)|^2 dz \quad (10)$$

$$|E^-(t+\Delta z, z_k)|^2 - |E^-(t, z_{k+1})|^2 = \int_{z_k}^{z_{k+1}} \left[N(t + z_{k+1} - z, z) - \beta\right] \times |E^-(t + z_{k+1} - z, z)|^2 dz \quad (11)$$

where at $\beta = 0$ the integrals on the right-hand side of (10) and (11) can be up to the order Δz^3 approximated by the two integrals from the right-hand side of (9). Therefore, using relations (7) and (8) together with (10) and (11) and the trapezoidal approximation to the integrals

$$-\beta\int_{z_k}^{z_{k+1}} |E^-(t + z_{k+1} - z, z)|^2 dz - \beta\int_{z_k}^{z_{k+1}} |E^+(t - z_k + z, z)|^2 dz$$

and assuming that $\beta\Delta z \ll 1$, we obtain

$$\frac{dG_k}{dt} = G_0 - \gamma G_k - s e^{-\beta\Delta z/2} \times \left(e^{G_k} - 1\right)\left[|E^+(t, z_k)|^2 + |E^-(t, z_{k+1})|^2\right]. \quad (12)$$

The system of coupled differential-algebraic equations (7), (8), and (12) approximates the evolution of the electric field envelopes and the carrier density in the gain and absorber sections. To solve these equations, we used the time discretization $\Delta t = \Delta z$, consistent with the space discretization, and an implicit numerical scheme for the differential (12). To describe the transformation of the amplitudes $E^{\pm}$ in the passive section, the algebraic relations (7) and (8) with $G_k = 0$ were used.

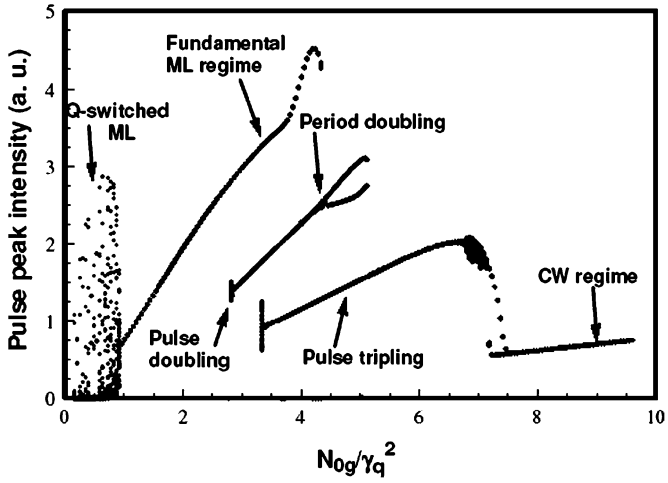

Fig. 2. Numerical bifurcation diagram illustrating different operation regimes of a monolithic mode-locked laser. $\alpha_g = \alpha_q = 0$.

IV. Bifurcation Diagrams

Fig. 2 presents a bifurcation diagram, which was obtained by the numerical solution of (7), (8), and (12) with boundary conditions (3) and (4). In this figure, local maxima of the intensity time traces $|E^+(t, L)|^2$ of the electric field amplitude at the right laser facet are plotted against the value of the control parameter N_{0g} corresponding to the unsaturated gain N_0 in the gain section. The unsaturated loss N_{0q} in the absorber section is fixed for Fig. 2. The sequences of bifurcations shown in these plots are in good qualitative agreement with the results obtained using the DDE mode-locking model [10]. For small injection currents (small N_{0g}), the mode-locking regime is unstable with respect to the Q-switching instability. In the unstable range, the amplitude of mode-locked pulses is slowly modulated with the Q-switching frequency $\Omega_Q \approx 3.4$ GHz (see Fig. 3). With the increase of the gain current, the fundamental mode-locking regime becomes stable. This regime corresponds to a sequence of short pulses with the repetition period close to the cavity round-trip time [see Fig. 4(a)].

With further increase of the injection current in the gain section, the fundamental mode-locking branch disappears after a saddle-node bifurcation and a sudden jump happens to a harmonic mode-locking regime with approximately twice higher repetition rate [see Fig. 4(b)]. This regime corresponds to a pair of mode-locked pulses counter-propagating in the cavity. This type of harmonic mode-locking regime was observed experimentally in a passively mode-locked monolithic semiconductor laser [12]. Within the framework of the DDE model based on the ring cavity approximation, the two pulses are always equidistant and have equal amplitudes [10]. As opposed to this approximation, in a linear laser, the branch of harmonic mode-locked pulses can exhibit the period doubling bifurcation leading to different pulse amplitudes and time separations [see Figs. 2 and 4(b)]. This bifurcation has a simple intuitive interpretation. Unlike pulses propagating unidirectionally in a ring laser, the two counterpropagating pulses in a linear cavity must collide in the course of their propagation. If the pulses emitted by the laser are identical and equally spaced in time, the collision takes place in the (optical) midpoint of the cavity. For the parameter values

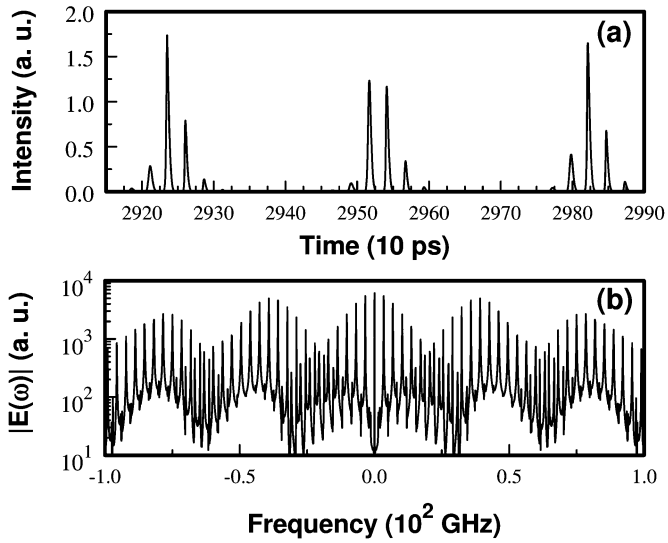

Fig. 3. Q-switched mode-locking regime. (a) Time trace of the electric field intensity $|E^+(t,L)|^2$. (b) Optical spectrum corresponding to the time trace shown in panel (a). $N_{0g} = 0.25\gamma_q^2$. Other parameters are the same as in Fig. 2.

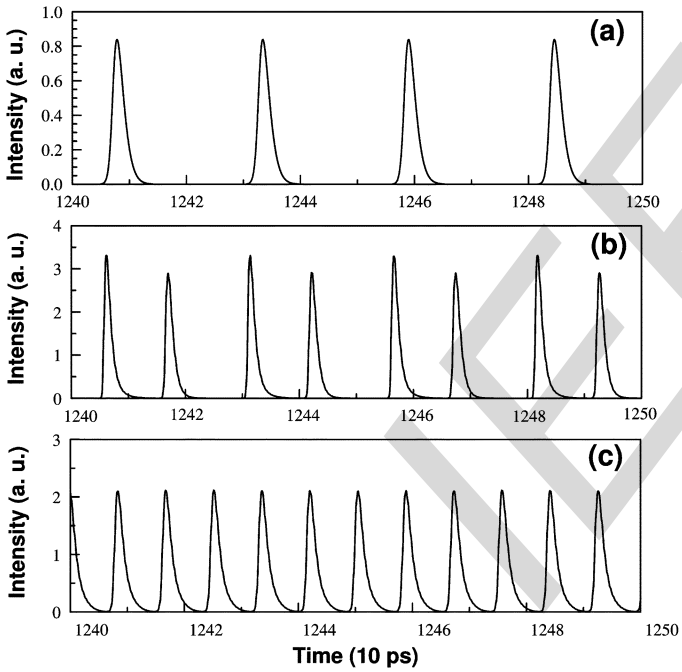

Fig. 4. Time traces of the laser intensity $|E^+(t,L)|^2$. (a) $N_{0g}/\gamma_q^2 = 0.96$, the fundamental mode-locking regime. (b) $N_{0g} = 5.0\gamma_q^2$, a harmonic mode-locking regime with two pulses in the cavity having different peak power and time separations. (c) $N_{0g} = 6.5\gamma_q^2$, a harmonic regime with three pulses in the cavity. Other parameters are the same as in Fig. 2.

used in our calculations this point is located inside the amplifying medium, not far away from the right end of the gain section. Hence, in this case the collision of two pulses should result in a strong local saturation in this section which is unfavorable for laser generation. On the other hand, for the regime shown in Fig. 4(b) with slightly different distances between the two consecutive pulses, only every second collision takes place in the gain section, while the other collisions occur in the phase tuning section. Therefore, the period-doubling bifurcation shown in Fig. 2 leads to a reduction of the gain section saturation. One

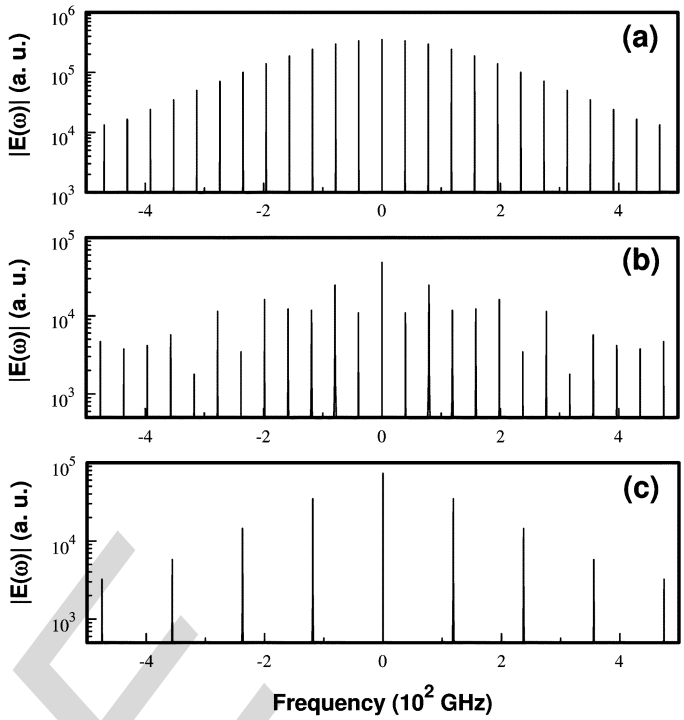

Fig. 5. Optical spectra corresponding to the regimes shown in Fig. 2. (a) $N_{0g} = 0.96\gamma_q^2$, the fundamental mode-locking regime. (b) $N_{0g} = 5.0\gamma_q^2$, a harmonic mode-locking regime with two pulses in the cavity having different peak power and time separations; (c) $N_{0g} = 6.5\gamma_q^2$, a harmonic regime with three pulses in the cavity. Parameters are the same as in Fig. 2.

could expect that similar bifurcation is responsible for assymmetry of pulse energies in a colliding-pulse mode-locked laser with an assymmetric design [22].

Harmonic mode-locked regimes with two pulses having different amplitudes and separations were recently observed experimentally in a monolithic quantum-dot laser [23]. However, since the device studied in this paper had only two sections, gain and absorber, the mechanism described above can hardly be used for interpretation of the observed differences in pulse amplitude and spacings. According to [27], a period-doubling bifurcation of the harmonic mode-locking regime in a quantum-dot laser can be explained in the framework of the ring cavity DDE model by taking into consideration carrier exchange processes between quantum dots and wetting layer.

Optical spectra of the fundamental and harmonic mode-locking regimes are presented in **[AUTHOR: PLEASE CITE FIGS. 5 AND 6 PRIOR TO FIG. 7.—ED.]** Fig. 7. For the harmonic mode-locking regime with $M = 3$ pulses coexisting in the cavity, only the modes with the numbers $m = 0, \pm M, \pm 2M, \ldots$ dominate in the spectrum [see Fig. 7(c)]. Due to the period-doubling bifurcation leading to different pulse amplitudes and separations, the suppression of the modes with the numbers $m \neq 0, \pm M, \pm 2M, \ldots$ is not so pronounced for the mode-locking regime with $M = 2$ shown in Fig. 7(b). However, as one could expect, in this regime the modes with the numbers $m = 0, \pm M$ have the largest amplitudes in the spectrum. In [24], the suppression of modes with odd numbers m was reported in a colliding-pulse mode-locked

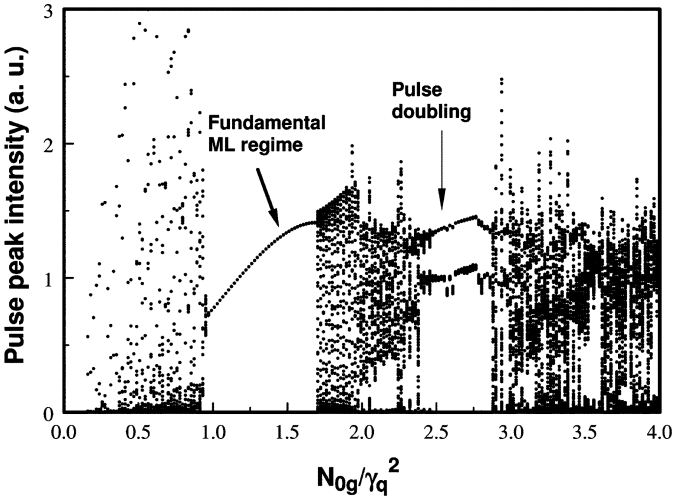

Fig. 6. Same as Fig. 2, but with nonzero linewidth enhancement factors, $\alpha_g = 2$ and $\alpha_q = 1$.

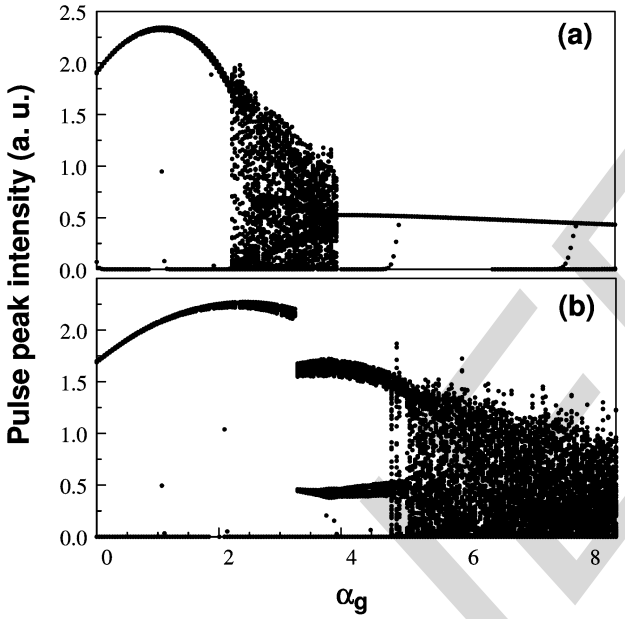

Fig. 7. Mode-locking pulse peak intensities for the varied linewidth enhancement factor α_g and fixed α_q. (a) $\alpha_q = 1$. (b) $\alpha_q = 3.5$. $N_{0g} = 3.0\gamma_q^2$.

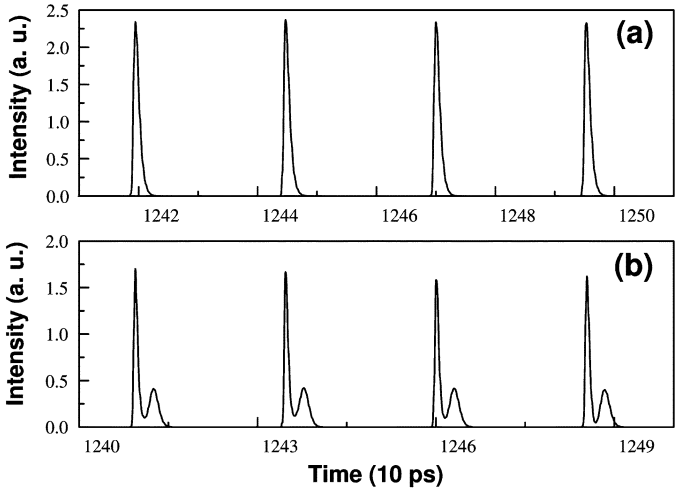

Fig. 8. Laser intensity time traces for different mode-locking regimes shown in Fig. 7. (a) Fundamental mode-locking regime for $\alpha_g = \alpha_q = 1$. (b) Quasi-periodic mode-locking regime with a satellite pulse behind the main pulse for $\alpha_g = \alpha_q = 3.5$. Other parameters are the same as in Fig. 7.

laser. We note that, according to the bifurcation diagram shown in Fig. 2, there exist wide ranges in the parameter space where the model equations exhibit bistability and even tristability between different types of mode-locking regimes. Similar multistability was observed experimentally in a passively mode-locked InGaAsP laser with an external mirror [21].

The numerical results presented in Figs. 2, 3, 4, and 7 have been obtained with the zero linewidth enhancement factors both in the gain and the absorber sections, $\alpha_{q,q} = 0$. Fig. 6 presents a diagram similar to that shown in Fig. 2, but corresponds to nonzero linewidth enhancement factors in both gain and absorber sections. It is seen from the figure that the inclusion of α-factors leads to a substantial degradation of mode-locking regimes. In particular, harmonic mode-locking regimes with high repetition rates are transformed into chaotic pulsations for sufficiently large $\alpha_{g,q}$. This can explain why it is quite difficult to observe harmonic mode-locking regimes in 40-GHz devices studied in [3]. Such regimes can be more easily achieved in longer monolithic devices, see, e.g., [23]. This is in agreement with the results of [11] where it was shown that increasing the laser cavity length favors the appearance of harmonic mode-locking.

Fig. 7 presents diagrams similar to those shown in Figs. 2 and 6 but obtained by using the linewidth enhancement factor α_g in the gain section as the bifurcation parameter. The effect of changing the linewidth enhancement factor α_g in the gain section on the fundamental mode-locking regime is illustrated by Fig. 7 obtained for a fixed value of the α-factor of the absorber section, which is $\alpha_q = 1$ and $\alpha_q = 3.5$ for Fig. 7(a) and (b), respectively. If follows from these figures that the maximal amplitude of mode-locked pulses is achieved when α-factors of the gain and absorber sections are approximately equal, i.e., $\alpha_g = \alpha_q$, which is in agreement with the result obtained with the DDE model describing a ring laser with unidirectional lasing [10]. Further increase of α_g leads to a gradual decrease of the amplitude of the mode-locked pulse and hence to a degradation of the mode-locking regime.

Intensity time traces and corresponding optical spectra of mode-locked regimes of (1) and (2) with nonzero linewidth enhancement factors are shown in Figs. 8 and 9. It is seen that the self-phase modulation introduced by the α-factor results in asymmetry of the emission spectrum. Similarly to the results of [24] this spectrum has steeper red edge. According to Fig. 7(b), at some critical value of the linewidth enhancement factor a sharp transition to a mode-locking regime with an additional small "satellite" pulse following the main pulse takes place (see Fig. 8). The amplitudes of both the pulses are slightly modulated in time, which implies that the regime shown in Fig. 8(b) corresponds to the laser intensity changing quasi-periodically in time rather than periodically. This is confirmed by the picture of the optical spectrum of this regime shown in the right panel of Fig. 9(b), where each of the laser modes is split into two lines with the frequency difference

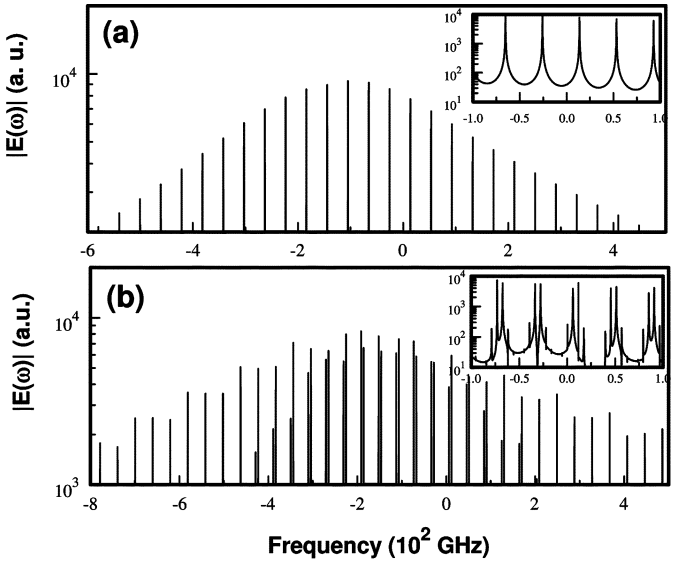

Fig. 9. Optical spectra for different mode-locking regimes shown in Fig. 8. (a) Fundamental mode-locking regime for $\alpha_g = \alpha_q = 1$. (b) Quasi-periodic mode-locking regime with a satellite pulse behind the main pulse for $\alpha_g = \alpha_q = 3.5$. Other parameters are the same as in Fig. 7.

$\Delta\Omega \approx 5.6$ GHz, i.e., approximately seven times smaller than the intermode frequency spacing $\Delta\omega \approx 39.6$ GHz. Regimes with additional small satellite pulses behind the main pulse are known to appear in external cavity passively (see, e.g, [25]) and actively mode-locked lasers [20], [26]. In [20], the asymmetric pulse shape and satellite pulse formation was explained by the dynamic detuning effect in active mode-locking. Here we demonstrate that a sharp transition to a similar type of regimes may appear due to the presence of α-factor responsible for strong carrier density dependency of the refractive index. Finally, we note that for the regime shown in Fig. 9(b) the amplitudes of the main and the satellite pulses oscillate with a very small amplitude near certain mean values. In a similar regime reported in [12], the amplitudes of the two pulses are strongly oscillating: the main pulse is transformed periodically into a satellite one and vice versa. Therefore, in the latter regime, a satellite pulse can exist both at the leading and the trailing edge of the main pulse.

V. Conclusion

To study dynamical instabilities in a passively mode-locked semiconductor laser, we have applied an efficient algorithm for numerical analysis of the traveling wave equations describing the space–time evolution of counterpropagating waves in this laser. The results of the numerical implementation of this algorithm appear to be in good qualitative agreement with those obtained with the DDE model describing unidirectional operation in a ring laser. In particular, multistability between the fundamental and different harmonic mode-locking regimes has been demonstrated for wide parameter ranges. However, numerical simulations revealed also certain differences between the two models. We have shown that, unlike the ring cavity DDE model, the one based on the traveling wave equations for counterpropagating waves in a linear cavity can exhibit a period doubling bifurcation of the harmonic mode-locking regime with two pulses in the cavity. This bifurcation, resulting in different amplitudes and separations of the two pulses, is related to the increased saturation of the gain section at the point where the counterpropagating pulses collide. We have studied the effect of the α-factors in the gain and absorber sections on the dynamics of the mode-locked laser and shown that the maximal intensity of mode-locked pulses is achieved when the α-factors in the two sections are approximately equal. A sharp transition to a quasi-periodic mode-locking regime with additional small satellite pulse following the main one is described.

Acknowledgment

The authors would like to thank D. Turaev, M. Radziunas, M. Wolfrum, and E. Viktorov for useful discussions.

References

[1] L. A. Jiang, E. P. Ippen, and H. Yokoyama, *Ultrahigh-Speed Optical Transmission Technology*. Berlin, Germany: Springer-Verlag, 2007, ch. Semiconductor mode-locked lasers as pulse sources for high bit rate data transmission, pp. 21–51***[Author: Please provide chapter number.--Ed.]***.

[2] R. Kaiser and B. Hüttl, "Monolithic 40-GHz mode-locked MQW DBR lasers for high-speed optical communication systems," *IEEE J. Sel. Top. Quantum Electron*, vol. 13, no. 1, pp. 125–135, Jan.–Feb. 2007.

[3] B. Hüettl, R. Kaiser, C. Kindel, S. Fidorra, W. Rehbein, H. Stolpe, G. Sahin, U. Bandelow, M. Radziunas, A. G. Vladimirov, and H. Heidrich, "Monolithic 40 GHz MQW mode-locked lasers on GaInAsP/InP with low pulse widths and controlled Q-switching," *Appl. Phys. Lett.*, vol. 88, no. 22, pp. 221104–221104, 2006.

[4] D. Rachinskii, A. G. Vladimirov, U. Bandelow, B. Hüttl, and R. Kaiser, "Q-switching instability in a mode-locked semiconductor laser," *J. Opt. Soc. Amer. B*, vol. 23, no. 4, pp. 663–670, 2006.

[5] Kuntz, G. Fiol, M. Lämmlin, D. Bimberg, M. G. Thompson, K. T. Tan, C. Marinelli, R. V. Penty, I. H. White, V. M. Ustinov, A. E. Zhukov, Y. M. Shernyakov, and A. R. Kovsh, "35 GHz mode-locking of 1.3 μm quantum dot lasers," *Appl. Phys. Lett.*, vol. 85, pp. 843–845, 2004.

[6] E. Viktorov, P. Mandel, A. G. Vladimirov, and U. Bandelow, "A model for mode-locking in quantum dot lasers," *Appl. Phys. Lett.*, vol. 88, pp. 201102–201102, 2006.

[7] E. Avrutin, J. Marsh, and E. Portnoi, "Monolithic and multi-Giga-Herz mode-locked semiconductor lasers: Constructions, experiments, models, and applications," *IEE Proc.-Optoelectron.*, vol. 147, pp. 251–278, 2000.

[8] A. G. Vladimirov, D. Turaev, and G. Kozyreff, "Delay differential equations for mode-locked semiconductor lasers," *Opt. Lett.*, vol. 29, pp. 1221–1223, 2004.

[9] A. G. Vladimirov and D. Turaev, "New model for mode-locking in semiconductor lasers," *Radiophys. Quantum Electron.*, vol. 47, no. 10-11, pp. 857–865, 2004.

[10] A. G. Vladimirov and D. Turaev, "Model for passive mode-locking in semiconductor lasers," *Phys. Rev. A*, vol. 72, pp. 033808–033808, 2005.

[11] M. Nizette, D. Rachinskii, A. G. Vladimirov, and M. Wolfrum, "Pulse interaction via gain and loss dynamics in passive mode-locking," *Physica D*, vol. 218, no. 1, pp. 95–104, 2006.

[12] U. Bandelow, M. Radziunas, A. G. Vladimirov, B. Hüttl, and R. Kaiser, "40 GHz modelocked semiconductor lasers: Theory, simulations and experiment," *Opt. Quantum Electron.*, vol. 38, no. 4, pp. 495–512, 2006.

[13] J. E. Caroll, J. E. A. Whiteaway, and R. G. S. Plumb, *Distributed Feedback Semiconductor Lasers*. London, U.K.: IEE/SPIE Opt. Eng. Press, 1998.

[14] U. Bandelow, M. Radziunas, J. Sieber, and M. Wolfrum, "Impact of gain dispersion on the spatio-temporal dynamics of multisection lasers," *IEEE J. Quantum Electron.*, vol. 37, no. 2, pp. 183–188, Feb. 2001.

[15] A. J. Lowery, "New dynamic semiconductor laser model based on the transmission line modelling method," *Proc. IEE*, vol. 135, pp. 126–126, 1988.

[16] R. J. Helkey, P. A. Morton, and J. E. Bowers, "Partial integration method for analysis of mode locked semiconductor lasers," *Opt. Lett.*, vol. 15, pp. 112–114, 1990.
[17] V. B. Khalfin, J. M. Arnold, and J. H. Marsh, "A theoretical model of synchronization of a mode-locked semiconductor laser with an external pulse stream," *IEEE J. Sel. Top. Quantum Electron.*, vol. 1, no. 2, pp. 523–527, Jun. 1995.
[18] L. Zheng, C. R. Menyuk, and G. M. Carter, "A realistic model for actively modelocked semiconductor lasers," *IEEE Photon. Technol. Lett.*, vol. 6, no. 2, pp. 167–169, Feb. 1994.
[19] J. Catherall and G. New, "Role of spontaneous emission in the dynamics of mode locking by synchronous pumping," *IEEE J. Quantum Electron.*, vol. QE-22, no. 8, pp. 1593–1599, Aug. 1986.
[20] K. Hsu, C. M. Verber, and R. Roy, "Stochastic mode-locking theory for external-cavity semiconductor lasers," *J. Opt. Soc. Amer. B*, vol. 8, pp. 262–275, 1991.
[21] M. Kuznetsov, D. Z. Tzang, J. N. Walpole, Z. L. Liau, and E. P. Ippen, "Multistable mode locking of InGaAsP semiconductor lasers," *Appl. Phys. Lett.*, vol. 51, pp. 895–897, 1987.
[22] D. Kuhlke, W. Rudolph, and B. Wilhelmi, "Calculation of the colliding pulse mode locking in CW dye ring lasers," *IEEE J. Quantum Electron.*, vol. QE-19, no. 4, pp. 526–533, Apr. 1983.
[23] E. A. Viktorov, P. Mandel, M. Kuntz, G. Fiol, D. Bimberg, A. G. Vladimirov, and M. Wolfrum, "Stability of the modelocking regime in quantum dot laser," *Appl. Phys. Lett.*, vol. 91, pp. 231116–231116, 2007.
[24] E. A. Avrutin, J. M. Arnold, and J. H. Marsh, "Dynamic modal analysis of monolithic mode-locked semiconductor lasers," *IEEE J. Sel. Top. Quantum Electron.*, vol. 9, no. 3, pp. 844–856, May–Jun. 2003.
[25] Y. Silberberg, P. W. Smith, D. G. Eilenberger, D. A. B. Miller, A. C. Gossard, and W. Wiegmann, "Passive mode-locking of a semiconductor diode laser," *Opt. Lett.*, vol. 9, pp. 507–509, 1984.
[26] S. Gee and J. E. Bowers, "Ultraviolet picosecond optical pulse generation from a mode-locked InGaN laser diode," *Appl. Phys. Lett.*, vol. 79, pp. 1951–1952, 2001.
[27] A. G. Vladimirov and D. I. Rachinskii, "Bifurcation analysis of a model of passively mode-locked quantum dot laser," in *Proc. SPIE Europe Photon. Europe*, Strasbourg, Germany, Apr. 7–10, 2008***[Author: Please provide page numbers.--Ed.]***.

Andrei G. Vladimirov was born in Leningrad (now St. Petersburg), Russia, in 1958. He received the Ph.D. and D.Sc. degrees from St. Petersburg State University, St. Petersburg, Russia, in 1984 and 2006, respectively.

He was a Researcher and, since 2000, and an Associate Professor with the Physics Faculty, St. Petersburg State University. Currently, he is with the Weierstrass Institute for Applied Analysis and Stochastics, Berlin, Germany, and the Department of General Physics, St. Petersburg State University. His research interests include nonlinear dynamics in semiconductor lasers and laser systems, localized structures, and pulses of light in fibers and broad-area lasers.

Alexander S. Pimenov was born in Samara, Russia, in 1983. He received the M.Sc. degree in applied mathematics from M. Nayanova University of Samara, Samara, in 2005. He is currently working toward the Ph.D. degree in applied mathematics at University College Cork, Cork, Ireland.

Dmitrii Rachinskii received the M.Sc. degree in mathematics and physics and the Ph.D. degree in mathematics from the Moscow Institute of Physics and Technology, Moscow, Russia, in 1994 and 1997, respectively, and the D.Sc. degree in applied mathematics from Institute of Control Problems, Russian Academy of Sciences, Moscow, in 2002.

He was a Researcher and a Postdoctoral Research Fellow with the Institute for Information Transmission Problems, Moscow, University of Regensburg, Germany, Technical University of Munich, and Weierstrass Institute for Applied Analysis and Stochastics, Berlin. Since 2005, he has been with the Department of Applied Mathematics, University College Cork, Cork, Ireland. His primary research interests are in the area of nonlinear dynamics and applied mathematical modelings, including phase locking in light-emitting devices and electronic circuits.